Available online at www.sciencedirect.com
ScienceDirect
Journal of Power Sources 176 (2008) 229–239
JOURNAL OF POWER SOURCES
www.elsevier.com/locate/jpowsour

Synergistic integration of a gas turbine and solid oxide fuel cell for improved transient capability

Fabian Mueller, Robert Gaynor, Allie E. Auld, Jacob Brouwer *, Faryar Jabbari, G. Scott Samuelsen

National Fuel Cell Research Center, University of California at Irvine, Irvine, CA, United States

Received 23 July 2007; received in revised form 18 October 2007; accepted 19 October 2007
Available online 4 November 2007

Abstract

A theoretical solid oxide fuel cell–gas turbine hybrid system has been designed using a Capstone 60 kW micro-gas turbine. Through simulation it is demonstrated that the hybrid system can be controlled to achieve transient capability greater than the Capstone 60 kW recuperated gas turbine alone. The Capstone 60 kW gas turbine transient capability is limited because in order to maintain combustor, turbine and heat exchangers temperatures within operating requirements, the Capstone combustor fuel-to-air ratio must be maintained. Potentially fast fuel flow rate changes, must be limited to the slower, inertia limited, turbo machinery air response. This limits a 60 kW recuperated gas turbine to transient response rates of approximately 1 kW s^{-1}. However, in the SOFC/GT hybrid system, the combustor temperature can be controlled, by manipulating the fuel cell current, to regulate the amount of fuel sent to the combustor. By using such control pairing, the fuel flow rate does not have to be constrained by the air flow in SOFC/GT hybrid systems. This makes it possible to use the rotational inertia of the gas turbine, to buffer the fuel cell power response, during fuel cell fuel flow transients that otherwise limit fuel cell system transient capability. Such synergistic integration improves the transient response capability of the integrated SOFC gas turbine hybrid system. Through simulation it has been demonstrated that SOFC/GT hybrid system can be developed to have excellent transient capability.
© 2007 Elsevier B.V. All rights reserved.

Keywords: SOFC/GT hybrid; Control design; System modeling; Comparison to data; Transient capability

1. Introduction and background

Solid oxide fuel cell gas turbine hybrid technology is being considered as a power alternative that achieves the goal of generating electric power at high thermal efficiency. The technology is being developed by companies such as Siemens, Mitsubishi Heavy Industry and Rolls Royce with government support [1–7]. Integrating a fuel cell and a gas turbine is by no means trivial and a significant system-level effort has been made to understand hybrid system integration and thermodynamics [8–17].

In hybrid systems the high temperature exhaust of the fuel cell is used to drive a gas turbine which provides the fuel cell air flow and supplementary power. Such synergistic integration makes it possible to achieve efficiencies greater then either technology is capable independently.

The few SOFC hybrid systems tested to-date have focused on demonstrating the technology and have been controlled in a very conservative manner. However, as the technology develops, it is important to quantify the transient capability of fuel cell gas turbine hybrid systems and understand the dynamics, controls, performance, and risks of hybrid transient capability. Improving the transient capability of stationary fuel cell systems can potentially improve the attractiveness of the technology because transient fuel cell systems are inherently more valuable then base loaded systems.

Fundamentally, the electrochemical response of fuel cells is rapid on the time scale of milliseconds. However, the response of other system components such as the gas turbine and fuel processor are on the order of seconds to tens of seconds. Differences between the fuel cell thermal response, gas turbine air response, fuel processor fuel flow response, and the fuel cell electrochemical response can lead to difficulties in main-

* Corresponding author. Tel.: +1 949 824 1999; fax: +1 949 824 7423.
E-mail addresses: fm@nfcrc.uci.edu (F. Mueller), rmg@nfcrc.uci.edu (R. Gaynor), aea@nfcrc.uci.edu (A.E. Auld), jb@nfcrc.uci.edu (J. Brouwer), fjabbari@uci.edu (F. Jabbari), gss@uci.edu (G.S. Samuelsen).

0378-7753/$ – see front matter © 2007 Elsevier B.V. All rights reserved.
doi:10.1016/j.jpowsour.2007.10.081

Nomenclature

C_V	constant volume specific heat capacity (kJ kmol^{-1} K^{-1})
H	enthalpy (kJ kmol^{-1})
J	moment of inertia (kg m^2)
M	mass (kg)
N	molar capacity (kmol)
$\dot{N}$	molar flow rate (kmol s^{-1})
P	pressure (kPa), power (kW)
$\dot{Q}$	heat transfer (kW), heat generated (kW)
R	universal gas constant (8.3145 J mol^{-1} K^{-1})
$\bar{R}$	species reaction rate (kmol s^{-1})
T	time (s)
T	temperature (K)
V	volume (m^3)
w	rotational velocity (rad s^{-1})
$\dot{W}$	rate of work (kW)
$\bar{X}$	species mole fraction (–)

Control variables

b	feedback contribution (–)
d	demand value (–)
e	error between feedback and set point value (–)
f	feed forward contribution (–)
FCP	fuel cell power (kW)
GTP	gas turbine power (kW)
N_{fc}	fuel flow rate (kmol s^{-1})
P	external power demand (kW)
r	reference set point value (–)
RPM	blower shaft speed (rpm)
tc	combustor temperature (K)
T_{stack}	fuel cell stack temperature (K)
u	system input (–)
y	system feedback value (–)

taining hybrid system operating requirements (as described in Table 1). However, with careful control system design, it is possible to manipulate SOFC/GT hybrid systems to obtain fast load following capability within system operating requirements.

It is critical to understand that fuel cells do not have a slow transient response characteristic. Rather, the challenge is to maintain the operating requirements of the system within all required constraints to enable rapid transient capability. Solid oxide fuel cell gas turbine hybrid systems are often believed to have poor transient load following capability in part because the few demonstrated hybrid systems have been very conservative and limited research has been conducted to realize and develop fuel cell hybrid transient capability. However, that does not mean that SOFC/GT hybrid systems cannot be developed to have rapid transient load following capability. To investigate and demonstrate the load following capability of both systems, a model of a Capstone 60 kW recuperated gas turbine has been developed and compared against experimental transient performance data. A hybrid system that integrates a solid oxide fuel cell

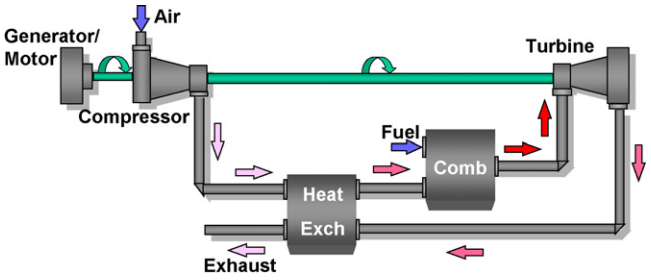

Fig. 1. Recuperated gas turbine schematic.

with a Capstone 60 kW gas turbine was developed and modeled. Both gas turbine and hybrid systems are designed, controlled, and simulated such that all system components are maintained within operating requirements. The modeling platform provides the ability to investigate aggressive fuel cell operation without damaging expensive prototype systems.

2. Systems

2.1. Capstone 60 kW micro-gas turbine

The Capstone 60 kW system is a recuperated micro-turbine generator (Fig. 1). The system uses a variable speed turbine to vary the amount of air through the system to keep the turbine exit flow temperature close to 910 K. This is the system critical temperature because the turbine exit is the hot exhaust recuperator inlet, which must be kept close to the maximum operating temperature with a small safety margin. By manipulating the air flow to maintain the turbine exit temperature, the heat exchanger inlet temperature and combustor temperature are consequently well maintained within operational constraints.

2.2. Solid oxide fuel cell gas turbine hybrid system

The Capstone gas turbine efficiency is in the range of 16–28%. To increase the system efficiency a solid oxide fuel cell can be integrated between the compressor and turbine as presented in Fig. 2. Integrating a gas turbine and fuel cell is synergistic because the compressor air flow is used by the fuel cell while the heat generated by the fuel cell can be used in the gas turbine to provide the compression energy as well as supple-

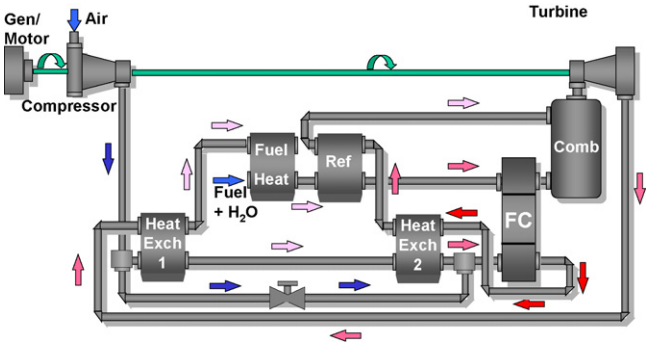

Fig. 2. SOFC gas turbine hybrid system without fuel or air recirculation schematic.

Table 1
Operating requirements of recuperated gas turbine and SOFC/GT hybrid system components

Concept	Value
Combustor (GT and hybrid)	
Sufficient air to fully oxidize fuel into the combustor	% Excess air >10%
Compressor (GT and hybrid)	
Avoid surge and choke	Maintain on map
Turbine (GT and hybrid)	
Maintain shaft speed to avoid turbine damage	Shaft speed <97000 rpm
Turbine inlet temperature must be maintained to avoid thermal degradation of turbine	TIT < 1600 K
Metal heat exchanger (GT and hybrid)	
Maintained heat exchanger maximum temperature to avoid heat exchanger thermal damage [38–40]	T < 950 K
Planar fuel cell (hybrid)	
Sufficiently high steam to carbon ratio to avoid carbon coking [17,40–42]	S/C > 2
Sufficiently high minimum MEA temperature for ionic conductivity	$T_{MEA} > 1000$ K
Limited MEA maximum temperature to avoid thermal degradation and MEA damage	$T_{MEA} < 1373$ K
Managed temperature gradient across the MEA to manage stresses caused by thermal gradients [17,41,43–45]	$\Delta T_{cathode} < 200$ K
Operating temperature should be maintained as close as possible to avoid thermal fatigue [17,40,43]	$\Delta T_{MEA} < 20$ K
Fuel cannot be depleted in the anode to avoid oxidation of anode electrode [17,41,46]	$U_{fuel} < 95\%$
Air cannot be depleted in the cathode to avoid reduction of the cathode electrode	$U_{air} < 30\%$
External reformer (hybrid)	
Sufficiently high steam to carbon ratio to avoid carbon coking	S/C > 2
Sufficiently high reformate exit temperature for methane conversion [17,45,47]	$T_{exit} > 900$ K
High temperature heat exchanger (hybrid)	
Maintained heat exchanger maximum temperature to avoid heat exchanger thermal damage [38–40]	$T < 1400$ K

mentary electrical power. As shown in the schematic of Fig. 2, integrating a fuel cell with the gas turbine is not trivial because of the stringent operating requirements as illustrated in Table 1.

A solid oxide fuel cell stack with 3220 10 cm × 10 cm anode supported planar cells (approximately 200 kW) was found to integrate well with the Capstone 60 kW micro-turbine. The primary design consideration for sizing the fuel cell was to match the gas turbine maximum air flow rate to maintain the fuel cell cathode temperature rise to within 150 K at high current densities. At maximum power the hybrid system generates 235 kW. Within the considered operating range between 135 and 235 kW, 70–82% of the system power is generated from the fuel cell (at a fuel cell efficiency ranging from 45 to 50%) and the balance generated from the gas turbine. Under these conditions the hybrid system efficiency is close to 60%, an efficiency greater than the fuel cell alone, and more than double that of the Capstone gas turbine.

In the system considered natural gas is reformed externally to the fuel cell, the cathode air is preheated to 1000 K and the air temperature rise through the fuel cell is kept within approximately 150 K to avoid large temperature gradients. To utilize the same components as those used to simulate the recuperated gas turbine, anode and cathode gas recirculation or flow splitting was not considered in the current hybrid cycle.

Ideally the turbine exit exhaust would contain sufficient heat to preheat the air and externally reform the fuel. However, while designing the system it was found that the turbine exhaust stream does not contain enough energy after expansion to provide all the heat required for reformation and air preheat at high fuel cell current density operation. At high current density, the turbine exit temperature is lower than the required fuel cell cathode inlet temperature. Consequently, the fuel and air were preheated to the extent possible using the turbine exhaust in the fuel heater and first air heat exchanger. Supplementary heat required for steam reformation and cathode air heating in the second air heat exchanger is supplied from the fuel cell cathode stream before the combustor. This ensures sufficient heat to both maintain high steam reformer temperature and cathode inlet temperature. Different strategies could have been used to ensure sufficient heat, including recirculation, partial oxidation of the inlet fuel, and recuperation from the combustor exhaust. The strategy implemented in this model is a design choice that resulted from the decision to recuperate heat between the fuel cell and the combustor. With sufficient heat the cathode inlet temperature can be controlled by manipulation of the bypass valve.

3. Model

The modeling methodology utilized herein has been used to develop models that compare well for dynamic single cell transients [18] as well as integrated simple cycle SOFC systems [19], SOFC/GT hybrid systems [20], and PEM stationary fuel cell systems [21]. Furthermore the modeling methodology has been used to investigate integrated fuel cell controls [14,16,19,22–24]. Because the modeling methodology and equations have been previously presented [14,16,18–27], the model will only be briefly described herein, but sufficient detail is provided to demonstrate the fidelity of the models used.

3.1. Discretization

The system dynamic models are developed in Simulink® using a methodology that develops a physical model for each of the primary system components: compressor, external steam reformers, heat exchanger, fuel cell stacks, combustors, and turbine. Each of the component models is then connected to represent the entire system. The dynamics of individual components as well as interactions amongst system components are captured to simulate the system dynamic response. The same compressor, turbine, combustor, and heat exchanger models are used in both systems.

Components are spatially discretized quasi-dimensionally using control volumes that convert partial differential equations into ordinary differential equations. The turbine, compressor, and combustor are each zero-dimensional models (discretized into a single control volume). The fuel cell is discretized into four control volumes: anode gas, electrode-electrolyte assembly, cathode gas, and separator plate. A detailed single SOFC cell model is taken as representative of all cells in the stack, with the flow and output scaled appropriately to predict full stack performance. The reformer and heat exchangers are discretized into several control volumes both in the cross-flow and in-flow directions in quasi-two-dimensional models. The reformer contains 9 control volumes and each heat exchanger contains 15 control volumes.

Resulting time ordinary differential equations for each control volume are then solved using Simulink® stiff differential equation solver ODE 15 s. Within each control volume only the physical and chemical processes that affect the time-scale of interest in the dynamic simulation are considered (>10 ms). Processes such as electrochemical reaction rates and electric current flow dynamics are assumed to occur at a time scale that is faster than that of interest to the model. Conservation equations and chemical kinetics are applied to each control volume. Transport phenomena such as ion and fluid flow and heat transfer are then resolved between control volumes.

3.2. Assumptions

Several assumptions are made in the development of the set of equations that is solved in each of the control volumes:

(1) Control volumes are characterized by a single lumped temperature, pressure, and species mole fractions condition.
(2) All gases are ideal gases.
(3) Gas mixtures are resolved for CH_4, CO, CO_2, H_2, H_2O, N_2, and O_2. All other species are assumed negligible for thermodynamics.
(4) No heat transfer to the environment. The system is assumed to be well insulated from the environment.
(5) Each cell in the stack is assumed to operate identically, so that a single SOFC cell simulation is taken as representative and used to calculate full stack performance [28,29].
(6) Quasi-steady electrochemistry is assumed, since the electrochemistry is rapid (on the order of 10^{-3} s) in comparison to the system transients of interest [30].
(7) Activation polarization in the anode is neglected. Activation polarization in the cathode is an order of magnitude higher than in the anode [31,32]. A single activation polarization equation is used to capture the effects of all physical and chemical processes that polarize the charge transfer process.
(8) In the fuel cell all reactants generate their ideal number of electrons and no fuel or oxidant crosses the electrolyte.

3.3. Governing equations

Each control volume exit temperature and species mole fraction is determined from the appropriate transient energy and species conservation equation of the same general form within various components of the system. Temperature at each gas control volume is evaluated from transient energy conservation equation in the form:

$$NC_V\frac{dT}{dt} = \dot{N}_{in}h_{in} - \dot{N}_{out}h_{out} + \sum \dot{Q}_{in} - \sum \dot{W}_{out} \quad (1)$$

Similarly the species mole fractions are determined from the vector species conservation equation as follows:

$$N\frac{d(NX_i)}{dt} = \dot{N}_{in}X_{i,in} - \dot{N}_{out}X_{i,out} + R_i \quad (2)$$

In the system some solid components must be resolved with specific geometric features to capture heat transfer, especially those separating two adjacent gas streams. The temperatures of solid nodal components can be determined from the solid energy conservation equation as follows:

$$\rho VC\frac{dT}{dt} = \sum \dot{Q}_{in} \quad (3)$$

From the species mole fraction and temperature of each state, the thermodynamic as well as transport properties between volumes can be readily determined to close the equation sets.

Conduction and convection heat transfer between nodes are found using Fourier's law and Newton's law of cooling, respectively, throughout the model. The reformer and fuel cell steam reformation kinetics are evaluated using the kinetic model presented by Xu and Froment [33,34]. The electrochemical reaction rate of hydrogen and oxygen is evaluated in the fuel cell from Faraday's law. The mass flow delay due to pressure transients in the fuel processing system are captured by evaluating the reformer exit flow from the orifice flow equation as explained in Beckhaus et al. [35] and Pukrushpan et al. [36].

$$\dot{N}_{out} = \dot{N}_o\sqrt{\frac{P_{in} - P_{out}}{\Delta P_o}} \quad (4)$$

where in the model the standard molar flow rate ($\dot{N}_o$) was evaluated as 1×10^{-6} kmol s^{-1}, the standard pressure drop (ΔP_o) was evaluated as 40 kPa, P_{out} is the fuel cell pressure deduced from the turbine pressure and P_{in} is the reformer pressure evaluated as:

$$\frac{dP}{dt} = \frac{RT}{V} \times \left(\dot{N}_{in} - \dot{N}_{out} + \sum R_i\right) \quad (5)$$

Note that flow delays associated with fuel actuators, desulfurizer, and steam generator are not physically resolved but are essentially lumped into the reformer mass flow delay.

The system is considered to be adiabatic, so the heat generated within the fuel cell and combustor is displaced by an increase in enthalpy of the flow. Energy of reactions is accounted for directly by considering both temperature and species dependent sensible enthalpies and all formation enthalpies.

The fuel cell voltage is evaluated as the local temperature, pressure, and species dependent Nernst potential minus activation, Ohmic, and concentration polarizations, where the fuel cell current is a controllable system input. The effective internal resistance is evaluated from [37] as:

$$R_{\text{eff}} = T_{\text{MEA}} \times \exp\left(\frac{7509.6}{T_{\text{MEA}}} - 25.85\right) \quad (6)$$

The turbine and compressor flow rate and efficiency are obtained from compressor and turbine maps based on the turbine shaft speed and pressure ratio. The system pressure is found from a system molar balance using the ideal gas law and solution of a dynamic pressure equation that accounts for mass storage in the volume, V, between the compressor and turbine as follows,

$$\frac{dP}{dt} = \frac{RT}{V}(\dot{N}_{\text{in,air}} + \dot{N}_{\text{in,fuel}} - \dot{N}_{\text{out}}) \quad (7)$$

This method captures volume effects of the gas turbine combustor and fuel cell. The turbine shaft speed is determined from the dynamic shaft momentum balance equation,

$$Jw\frac{dw}{dt} = P_{\text{turbine}} - P_{\text{compressor}} - P_{\text{generator}} \quad (8)$$

where the generator power is a manipulated input that is varied to control the gas turbine shaft speed and the compressor and turbine power are determined from isentropic relations and the compressor and turbine efficiency maps. Important model parameters are provided in Table 2.

Table 2
Important model parameters

Planar SOFC	
Number of planar anode supported fuel cells	3220
Exchange current density	4000 A m^{-2}
Limiting current density	9000 A m^{-2}
Width of cell	0.1 m
Length of cell	0.1 m
Depth of bulk gas channels	0.002 m
Thickness of MEA	0.001 m
Thickness of gas separator plate	0.0015 m
MEA density	5000 kg m^{-3}
MEA specific heat capacity	0.8 kJ kg^{-1} K^{-1}
Separator plate density	7900 kg m^{-3}
Separator plate specific heat capacity	0.640 kJ kg^{-1} K^{-1}
Steam reformer	
Number of reformer channels	1400
Thickness of reformer bed channels	0.01 m
Width of reformer channels	0.1 m
Length of reformer	0.3 m
Thickness of reformer exhaust channel	0.01 m
Catalyst bed density	1177.5 kg m^{-3}
Combustor	
Length	0.25 m
Diameter	0.25 m
Air recuperator	
Number of air ceramic heat exchanger channels in hybrid	40
Number of air metal heat exchanger channels in hybrid	50
Number of air metal heat exchanger channels in gas turbine	50
Number of fuel recuperator channels	84
Width of recuperator channels	0.1 m
Length of recuperator channels	10 m
Height of gas recuperator gas channels	0.01 m
Thickness of recuperator plates	0.0015 m
Plate conduction heat transfer coefficient	0.287 kW m^{-1} K^{-1}
Plate specific heat capacity	0.475 kJ kg^{-1} K^{-1}
Plate density	3970 kg m^{-3}

4. Recuperated gas turbine load following

4.1. Control development for modeled capstone system

The Capstone control strategy was unknown, so new controls were developed to maintain the system operating conditions. Developing a control strategy for the system provided insight into the transient capability of the system. The primary gas turbine system constraint is maintenance of a turbine exit (recuperator inlet) temperature below the maximum heat exchanger temperature during transient operation. Two system parameters can be manipulated in the gas turbine: the power drawn from the generator and the amount of fuel provided to the system. During operation it is critical to maintain the turbine exit temperature below the maximum heat exchanger temperature, or else the recuperator materials will begin to fail (melt). Due to this operating constraint, the transient load following capability of the recuperated gas turbine must be limited. The turbine exit temperature is affected by (1) the air flow rate through the system, (2) the amount of fuel combusted, and (3) the expansion of the exhaust in the turbine. To maintain the turbine exit temperature, the fuel flow to the combustor has to be approximately proportional to the air flow, which would produce conditions of roughly equivalent fuel-to-air ratios for all operating conditions. The air flow rate, which is roughly proportional to the shaft speed, can be controlled by manipulating the power demand. During an increase in power demand the goal of the control system is to increase the power generated by the turbine while maintaining the turbine exit temperature. If the generator power is increased too rapidly, the shaft speed and consequently the air flow rate will drop. If the air flow rate is reduced, then the fuel flow rate cannot be increased without causing the turbine exit temperature to rise to unacceptable values. Therefore, the system controller will need to limit the rate at which the power demand can increase in order to prevent excessive turbine inlet temperatures.

A decentralized controller was implemented in the model. The turbine exit temperature is controlled by manipulating the combustor fuel flow rate with a proportional and integral temperature feedback without feed forward. The gas turbine power control is based on a power demand and gas turbine shaft speed

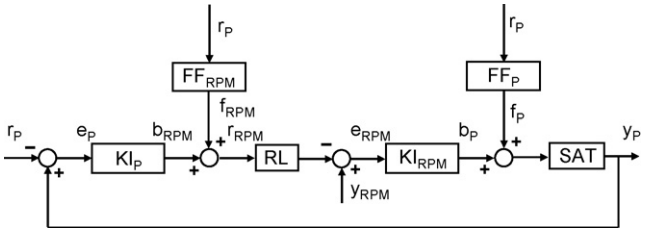

Fig. 3. Modeled 60 kW gas turbine power cascade controller.

cascade controller as shown in Fig. 3. A rate limit (RL) is used to limit how fast the turbine shaft speed is increased. Different gas turbine shaft speed ramp rates can be achieved depending on the amount of the gas turbine power allocated to speed up the turbine. Control parameters for the modeled Capstone controllers are presented in Table 3.

4.2. Model comparison to experimental data

To garner intuition into the transient capability of a recuperated gas turbine system and to increase confidence in the dynamic model, the Capstone model was compared to experimental data. The transient response of the Capstone 60 kW recuperated gas turbine model was compared to that of a commercial unit operated at the University of California, Irvine during an instantaneous 23–53 kW load demand increase. The power response to the instantaneous load demand increase of the commercial gas turbine system is shown as the solid line in Fig. 4. The turbine power output and shaft speed were measured and observed to ramp-up in unison during a load demand increase perturbation. The turbine power ramp rate is approximately linear at 1 kW s^{-1} while the turbine shaft speed ramps linearly at a rate of approximately 800 rpm s^{-1}. The turbine shaft

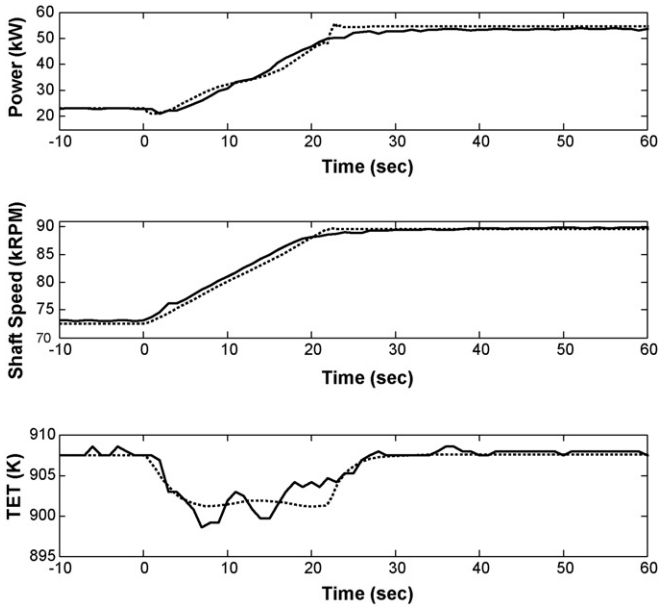

Fig. 4. Capstone 60 kW model (dotted line) comparison to experimental data (solid line) for an instantaneous 23–53 kW load demand increase.

speed increases in a more linear fashion than the gas turbine power, indicating that the turbine shaft speed is probably limited instead of the gas turbine generator power.

To compare the transient response of the model to the experimental data, the gas turbine shaft speed ramp rate limit was set to 800 rpm s^{-1} in the model control strategy. The modeled system response is plotted with the experimental gas turbine response in Fig. 4. Overall, the model power, shaft speed, and turbine exit temperature response compare well to the experimental response.

Table 3
Important control parameters

Modeled 60 kW GT power cascade controller		
K_P	100 rpm kW^{-1}	System power feedback proportional gain
I_P	0.2 rpm kW^{-1}	System power feedback integral gain
K_{RPM}	1×10^{-2} kW rpm^{-1}	Shaft speed feedback proportional gain
I_{RPM}	5×10^{-7} kW rpm^{-1}	Shaft speed feedback integral gain
Sat.	>0 kW	Gas turbine power saturation
Modeled 60 kW GT feedback controller (no feedforward)		
K_{Fuel}	5×10^{-7} kmol s^{-1} kW^{-1}	Fuel flow feedback proportional gain
I_{Fuel}	6×10^{-7} kmol s^{-1} kW^{-1}	Fuel flow feedback integral gain
Hybrid system GT power demand cascade controller		
K_{Tstack}	5000 rpm K^{-1}	Temperature feedback proportional gain
K_{RPM}	0.0133 kW rpm^{-1}	Shaft speed feedback proportional gain
Sat.	>0 kW	Gas turbine power saturation
System fuel flow fuel cell power controller		
K_{Fuel}	3×10^{-6} kmol s^{-1} kW^{-1}	Fuel flow feedback proportional gain
I_{Fuel}	1×10^{-7} kmol s^{-1} kW^{-1}	Fuel flow feedback integral gain
Fuel cell current combustor temperature controller		
$K_{Current}$	1.5 A K^{-1}	Current feedback proportional gain
$I_{Current}$	0.0133 A K^{-1}	Current feedback integral gain
Cathode inlet temperature controller		
K_{Bypass}	0.05 K^{-1}	Recuperator bypass feedback proportional gain
I_{Bypass}	5×10^{-4} K^{-1}	Recuperator bypass feedback integral gain

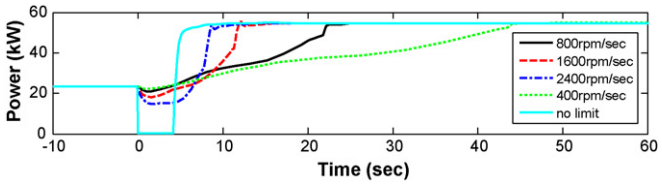

Fig. 5. Simulated gas turbine power response to an instantaneous 23–53 kW load demand increase for different gas turbine shaft speed ramp rates.

4.3. Sensitivity analysis

A sensitivity analysis was conducted to investigate the affect of the turbine shaft speed ramp rate limit on the turbine power response by varying the rate limit implemented in the controller. The gas turbine power responses to varying ramp rate limits are plotted in Fig. 5. For faster shaft speed ramp rates the gas turbine power does not ramp-up initially. Instead, the turbine power initially drops for high ramp rates. When the turbine ramp rate is not limited, the generator power drops to zero as the turbine speed increases. This is because the power supplied by the turbine is needed to accelerate the shaft. Faster gas turbine ramp rates allow the turbine to reach the new steady state faster, but the rise time is still fundamentally limited by the power needed to accelerate the shaft inertia. The gas turbine inherently required 5 s to reach steady state when there was no limit imposed on the turbine ramp rate. Note that in all cases the turbine exit temperature is well controlled by the manipulation of fuel flow to the combustor in the independent control loop as explained.

5. Hybrid load following

High temperature fuel cells can be synergistically integrated with gas turbine technology in hybrid systems that can produce electricity at high fuel-to-electricity conversion efficiencies with low emissions. The possible synergies associated with dynamic response characteristics and controls of integrated hybrid systems are not as well understood. To investigate the possible synergistic integration of a gas turbine with a solid oxide fuel cell to enhance load following capabilities, an appropriate control scheme must be developed and tested.

5.1. Decentralized control loops

The primary control limitation of the recuperated gas turbine was the recuperator inlet temperature. In the hybrid system, there are several other important constraints including (1) the fuel cell inlet and outlet temperature, (2) the combustor temperature and (3) sufficient fuel for the fuel cell, which must be maintained within acceptable limits. Along with the added constraints, the hybrid system comprises more inputs to the system that can be manipulated, including: (1) the amount of current drawn from the fuel cell, (2) system fuel flow (3) gas turbine power, and (4) the amount of air bypassing the recuperator. Depending on the requirements for cost, performance and durability, a variety of strategies can be used to control the system to meet all constraints during transient operation.

In the recuperated gas turbine, the transient capability of system must be limited to control the turbine exit temperature with a time scale that is constrained by how quickly the turbo-machinery can change speed for a given inertia. The hybrid system introduces additional degrees of freedom that allow development of control strategies that enhance the transient load-following characteristics. In the present work, a novel decentralized controller is investigated whereby the hybrid system combustor temperature (and consequently the turbine exit temperature), which was found to be problematic in the recuperated gas turbine system, is controlled by manipulating the fuel cell current. The fuel flow is then manipulated to control the fuel cell power, the fuel cell current is manipulated to control the combustor temperature, the gas turbine power is manipulated to control the fuel cell temperature by varying the air flow rate, and the recuperator bypass is manipulated to control the fuel cell inlet temperature. A similar approach has been previously investigated and discussed in detail in by Mueller et al. [24] for simple (non-hybrid) SOFC systems.

5.1.1. Combustor temperature control

The control approach implemented is particularly attractive because it allows the combustor temperature to be controlled without changing the system air flow. Such hybrid control makes it possible to avoid thermal constraints associated with the slow time response of the gas turbine air flow (or turbine shaft speed), which cannot be avoided in the recuperated gas turbine. This is possible because the amount of fuel entering the combustor can be independently manipulated by consuming more or less fuel in the fuel cell by changing the fuel cell current, which can be manipulated rapidly. Because the thermal capacitance of the fuel cell is large, the fuel cell can temporarily absorb additional heat generation from the current increase until the air flow rate increases to reject the additional heat generation. The fuel cell current combustor temperature controller is based on a feedforward steady state look up table with proportional and integral feedback gains as presented in Table 3.

5.1.2. Gas turbine fuel cell temperature controller and power buffering

The fuel cell temperature is controlled via the gas turbine cascade controller as presented in Fig. 6. Note that the gas turbine power cascade controller (Fig. 3) and the fuel cell temperature cascade controller (Fig. 6) are almost identical in structure. The key difference is that the fuel cell temperature controller does not use integral feedback to avoid integral windup due to the

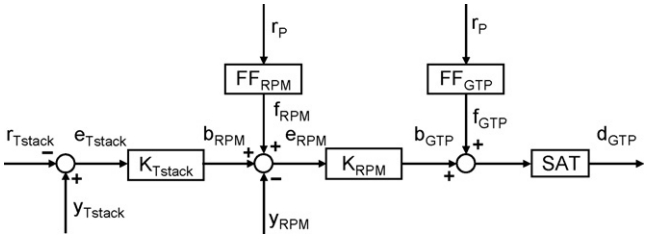

Fig. 6. Modeled hybrid system gas turbine power demand cascade controller.

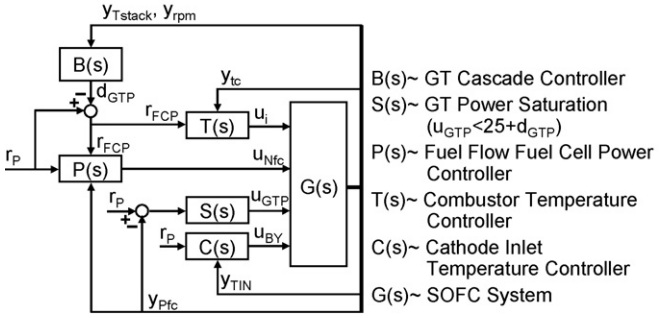

Fig. 7. Hybrid system integrated decentralized controller.

slow fuel cell thermal response. Control gains for the cascade controller are presented in Table 3.

Another novel aspect of the current control approach involves use of the gas turbine inertia as a slight energy buffer for the fuel cell in the hybrid system. The fuel flow rate entering the anode will be limited due to flow transients within the fuel preprocessor. Delays in the fuel flow rate will limit the ability of the fuel cell to respond to increases in power demand since increasing the current may consume fuel faster than it can be supplied. Since it takes time for the fuel to reach the fuel cell and the combustor the turbine inertia is used to temporarily produce more power (at the expense of shaft speed) to meet the overall power demand while the fuel cell power ramps up only as fuel is available. To implement this control approach, the SOFC power demand is set to be the system power demand minus the gas turbine power demand from the cascade controller. The actual gas turbine power then becomes the difference in power between the system power demand and the actual SOFC power (instead of that originally determined by the cascade controller). When the fuel cell power matches demand, the turbine power cascade controller demand and system power demand will also track set points. However, when the fuel cell power demand is not tracked, the power shortfall is provided by the turbine (inasmuch as it can provide such by use of stored rotational energy) so that the total system power demand is tracked. Sensitivity analyses showed that to prevent the gas turbine from stalling when the fuel cell power error is large, the gas turbine power demand must not exceed 25 kW. This 25 kW saturation level has been included in the control strategy resulting in the full set of decentralized controllers that are integrated as shown in Fig. 7.

5.2. Integrated system control

When perturbed, the hybrid system is moved to a new operating point by means of feedforward control and fuel cell power tracking. Feedback is used to maintain the system within all operating requirements during the transient. It is important that the time scale of each actuator is faster than the response time of the controlled variable to allow for adequate control. Overall the fuel cell power is tracked by manipulating the fuel flow. Small errors between the fuel cell power and its set point, which are due to fuel flow delay in the fuel processing system, are temporarily buffered by the gas turbine power when needed. As the fuel cell is enabled to meet the power demand transient (i.e., as fuel becomes available in the anode compartment), the gas turbine power is manipulated to control the fuel cell temperature via changes in air flow rate. The amount of fuel consumed within the fuel cell (or fuel utilization) is not controlled directly; however the combustor temperature is significantly and quickly affected by the fuel content exiting the fuel cell. Change in the fuel cell exit fuel concentration can be observed in the combustor temperature faster than the time scale of fuel depletion in the fuel cell. Even though the electrochemical time scale of the fuel cell is fast in the order of milliseconds, the time scale of fuel depletion in the fuel cell is in the order of seconds, which is longer than the thermal time scale of the combustor. For safety, the current response of the fuel cell can be slightly slowed down or governed to avoid low voltage conditions that occur as the anode compartment fuel is depleted.

In this control strategy the hybrid system has been synergistically integrated and controlled with the express purpose of enhancing dynamic response capabilities. Individual components are controlled to maintain all operating constraints while using rapid transient response characteristics of each component to compensate for limitations of other components. The large fuel cell thermal capacitance and ability to vary the fuel reaction rate rapidly through current manipulations are used to control the combustor temperature, which is an important operating constraint that rapidly responds to combustor fuel flow rate. Following a load increase, the gas turbine inertia is used to buffer the fuel cell during the short time when the fuel cell power ramps and sufficient fuel is not available in the anode compartment. That is, gas turbine rotating inertia can be temporarily harvested to compensate for fuel cell fuel delivery delays. Temporarily harvesting gas turbine power in this manner is acceptable, because even though the turbine shaft speed is decreased, the fuel cell thermal capacitance is large enough to enable fuel cell temperature control throughout the transient by subsequent increases in air flow. Furthermore, by temporarily decreasing the air flow, the combustor temperature controller manipulates the fuel cell current to cause increased fuel cell power (consistent with the demand increase). This control strategy is particularly attractive because the fuel cell is used to manage the primary limitation of the gas turbine transient capability (i.e., combustor temperature constraint), while the gas turbine is used to manage the primary limitation of the fuel cell transient capability (i.e., fuel delivery to the anode compartment)!

5.3. Simulation results

To demonstrate the load following capability of the system, a very large and rapid 100 kW s^{-1} system load demand transient from 135 to 235 kW was simulated in the hybrid system model with controls implemented as described above. Simulation results are shown in Figs. 8–10. The entire system tracks the load increase in approximately 20 s. The fuel cell can meet its new power demand in less than one second. The fuel cell cannot track load changes exactly because of the fuel delivery time delay. The system power demand is tracked initially because the gas turbine power buffers the slight tracking error of the fuel cell power. However, the gas turbine power saturates at 25 kW. For

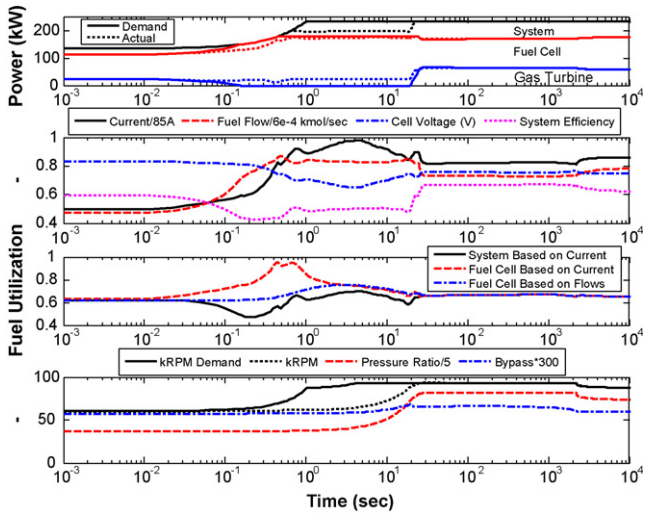

Fig. 8. Controlled hybrid system non-thermal response to a 100 kW s^{-1} system load demand from 135 to 235 kW.

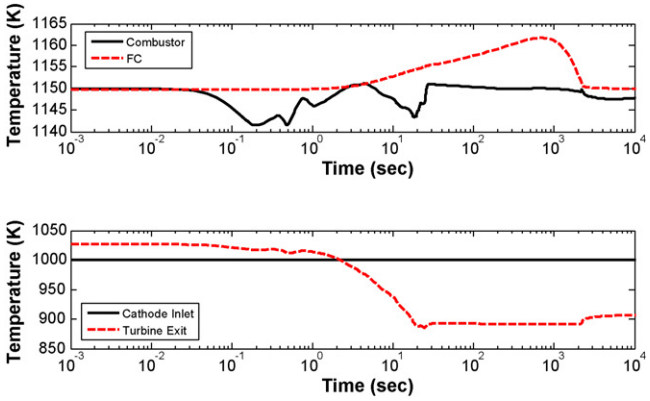

Fig. 9. Controlled hybrid system thermal response to a 100 kW s^{-1} system load demand from 135 to 235 kW.

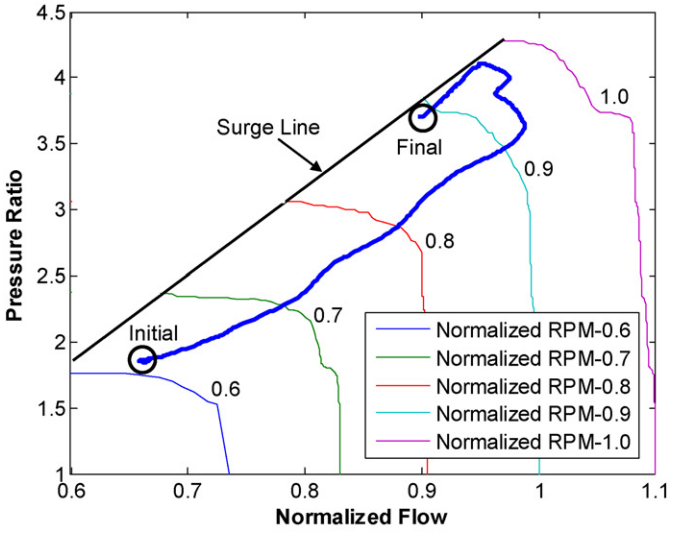

Fig. 10. Gas turbine compressor map, showing compressor path (bold line) for the controlled system 100 kW s^{-1} system load demand from 135 to 235 kW.

this large power transient from 135 to 235 kW, the system power could not be tracked during the 20 s it took the gas turbine shaft speed to increase. The gas turbine power was saturated and the fuel cell power was maximized. Note that the system power was tracked from 135 to 200 kW, but then took 20 s to increase from 200 to 235 kW due to the slower gas turbine transient response.

5.3.1. Maintaining operating requirements

The hybrid system control strategy is shown to be effective, but not capable of completely tracking the very large and rapid transient from 135 to 235 kW. Nonetheless, during the simulation the fuel cell voltage was maintained above 0.6 V $cell^{-1}$ (Fig. 8), fuel was not depleted within the fuel cell (Fig. 8), the combustor temperature was maintained within 10° (Fig. 9), the fuel cell inlet temperature remained within a degree (Fig. 9), and the fuel cell temperature was maintained within 15° (Fig. 9). The compressor operating regime is plotted on the compressor map in Fig. 10, indicating that the compressor did not surge or stall during the transient. The system was maintained within all operating requirements. The fuel flow and current increased concurrently without saturation to maintain the fuel cell power and combustor temperature. The gas turbine shaft speed increased rapidly during the major load change, even though the turbine provided some energy buffer for the fuel cell and the recuperator bypass did not saturate.

5.3.2. Explanation of system transient response

Controlling the system transient response is not trivial due to coupling among system components and decentralized control loops of various time scales. Initially when the system power demand is ramped, the feedforward terms in the system controller will cause the fuel cell power demand, fuel cell current, and system fuel flow rate to increase. However, the fuel flow does not instantaneously increase in the fuel cell due to fuel flow delay in the fuel processing system. Hence, the fuel cell power demand is not tracked and fuel within the anode compartment starts to deplete, causing an increase in fuel cell-fuel utilization (evaluated from the fuel cell anode inlet fuel flow and fuel cell current), even though the system global utilization (evaluated from the system inlet flow rate and fuel cell current) decreases.

$$U = \frac{i}{\dot{N}_{\text{in}}(4X_{\text{CH}_4} + X_{\text{CO}} + X_{\text{H}_2})_{\text{in}}} \tag{9}$$

During the fuel flow transient, fuel stored within the fuel cell provides a slight buffer for the fuel flow transient. The fuel cell-fuel utilization defined by the ratio of potential hydrogen in the anode exit stream to the potential hydrogen in the anode inlet stream.

$$U = 1 - \frac{\dot{N}_{\text{out}}(4X_{\text{CH}_4} + X_{\text{CO}} + X_{\text{H}_2})_{\text{out}}}{\dot{N}_{\text{in}}(4X_{\text{CH}_4} + X_{\text{CO}} + X_{\text{H}_2})_{\text{in}}} \tag{10}$$

Which accounts for stored fuel within the fuel cell, remained within acceptable values (Fig. 8). This indicates, fuel stored within the fuel cell, provides a sufficient buffer to avoid fuel depletion within the fuel cell. It is important to note that utilization evaluated from current represents steady state utilization

and utilization evaluated from the inlet and outlet flow represents transient utilization. At steady state both utilization will be equivalent, but during transients, the utilizations can be different due to stored fuel within the fuel cell.

With increased fuel utilization and increased fuel cell current, the fuel cell voltage dipped slightly. This resulted in a decrease in the fuel cell power. This tracking error in fuel cell power causes the feedback control to increase the fuel cell fuel flow, decreasing the system global utilization based on current.

The gas turbine speed takes on the order of seconds to increase. During the gas turbine transient, the fuel cell current is increased to maintain the combustor temperature. Once the gas turbine shaft speed is increased, the combustor is further cooled and the fuel cell current decreases. When the gas turbine shaft speed increased, the turbine power was recovered, which allowed the system power to be tracked and the fuel cell power to be decreased. With the increase in gas turbine power, the fuel cell power demand decreased resulting in a decrease in the fuel cell fuel flow.

The fuel cell temperature responded to the system power increase within seconds, and increased for minutes as heat within the fuel cell, heat exchangers, and reformer equilibrated. In effect, the fuel cell temperature rise after the gas turbine shaft accelerated is a result of thermal transients within the recuperator and reformer, which slightly decreased in temperature at higher system power. During the transient the cathode inlet temperature was well maintained by bypassing air around the recuperator. The turbine exit temperature was also well maintained. The turbine exit temperature decreased slightly due to a rise in operating pressure at high power operation, resulting in increased expansion cooling in the turbine.

Because the fuel cell current, system fuel flow, fuel cell power, and combustor temperature are all inter-coupled, flow delay in the fuel preprocessor, fuel consumption within the fuel cell, and controller actuation transients affect the entire system. It may be beneficial to utilize centralized controllers for these faster coupled control loops to avoid fast time scale transients, which were observed in the simulation due to component and decentralized control loop interactions.

6. Summary and discussion

The system transient performance is a result of the careful system integration and synergistic control design. Along with the transient capability that the hybrid system can achieve, the simulated system achieved efficiency greater than 60% at steady state and efficiencies greater than 40% throughout the transients. The transient capability of fuel cells and turbines are each limited by the balance of plant that is required to maintain the system within operating requirements. The Capstone 60 kW variable speed recuperated gas turbine had to maintain the fuel to air ratio and the gas turbine transient capability was thus constrained to rates at which the turbine shaft speed could be changed to maintain the recuperator temperature. This resulted in a system transient capability that was approximately 1 kW s^{-1} due to the turbo-machinery inertia. The fuel cell, on the other hand, is fundamentally constrained by the rate at which electrochemically active fuel constituents can be delivered to the anode compartment.

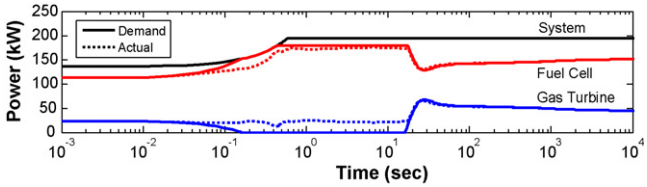

Fig. 11. Controlled hybrid system, fuel cell, and gas turbine power response to a 100 kW s^{-1} system load demand from 135 to 195 kW.

To create a hybrid system, a fuel cell, steam reformer, and heat exchangers were added to the turbine system. The added hardware represents both new operating requirements (Table 1) as well as new manipulated variables. With careful system integration and control considerations, the new variables can be used in control strategies that improve the hybrid system transient capability (above that which can be achieved by either the fuel cell or gas turbine alone) while maintaining the system within all operating requirements. When the system power demand is within the fuel cell maximum power limit, the turbine can buffer the fuel cell transient capability, which allows hybrid systems to have very rapid load following capability. This is demonstrated in Fig. 11 showing the system, fuel cell, and gas turbine power response to a large and rapid 100 kW s^{-1} hybrid load increase from 135 to 195 kW. Note that for this perturbation, the system was able to completely track power demand and simultaneously maintain all critical operational parameters.

The potential to synergistically integrate and control a hybrid fuel cell gas turbine system for rapid transient load following capability has been identified. Hybrid systems operating within the power range of the fuel cell should be able to track large and rapid power demands using the gas turbine as an energy buffer. Further control analysis in terms of disturbance rejection and efficiency should be conducted as well as analysis investigating the durability and transient capability of hybrid systems. The transient capability of the SOFC system should also be experimentally verified. Future hybrid system control can include development of centralized control to improve disturbance rejection, gas turbine surge protection for turn down, and simulation demonstration of hybrid system to load data.

7. Conclusions

The operating requirements of hybrid fuel cell gas turbine systems are more stringent than those for recuperated Brayton cycles. Consequently, hybrid systems will require a more sophisticated control system than gas turbine systems. However, with properly implemented controls and hybrid system integration, the system can be maintained within all operating requirements. Dynamic simulations indicate SOFC/GT hybrid systems can be developed to have rapid transient load following capability that is faster than that of recuperated gas turbines.

Because of the strict operating requirements, first generation hybrid systems may not have rapid transient load following capability. However, the current work shows that rapid tran-

sient capabilities are possible, which should inspire confidence in hybrid system controls that will enable future generation hybrid systems with rapid transient capabilities. Rapid transient capability could become economically valuable by enabling installation to meet a wide variety of power demands without energy storage or adverse grid impacts. The current dynamic simulations indicate hybrid systems can be developed to have transient capability surpassing those of gas turbine systems. This could potentially be used as a technical advantage for hybrid systems that has not previously been considered.

References

[1] M.C. Williams, J.P. Strakey, W.A. Surdoval, J. Power Sources 143 (1–2) (2005) 191–196.
[2] M.C. Williams, J.P. Strakey, S.C. Singhal, J. Power Sources 131 (1–2) (2004) 79–85.
[3] M.C. Williams, J. Strakey, W. Sudoval, J. Power Sources 159 (2) (2006) 1241–1247.
[4] SECA wraps first phase with SOFCs on way to commercial reality, Fuel Cells Bull. 2007 (7) (2007) 4.
[5] Siemens SOFC system exceeds DOE objectives, Fuel Cells Bull. 2007 (1) (2007) 5–6.
[6] Euro funding for Rolls-Royce SOFC hybrid, Fuel Cells Bull. 2003 (11) (2003) 4–5.
[7] Mitsubishi develops Japan's first SOFC-MGT system, Fuel Cells Bull. 2006 (10) (2006) 4.
[8] A. Franzoni, L. Magistri, A. Traverso, A.F. Massardo, Energy, in press.
[9] P.G. Bavarsad, Int. J. Hydrogen Energy, in press.
[10] W.-H. Lai, C.-A. Hsiao, C.-H. Lee, Y.-P. Chyou, Y.-C. Tsai, J. Power Sources 171 (1) (2007) 130–139.
[11] S.K. Park, K.S. Oh, T.S. Kim, J. Power Sources 170 (1) (2007) 130–139.
[12] J. Milewski, A. Miller, J. Salacinski, Int. J. Hydrogen Energy 32 (6) (2007) 687–698.
[13] J.S. Yang, J.L. Sohn, S.T. Ro, J. Power Sources 166 (1) (2007) 155–164.
[14] F. Mueller, F. Jabbari, J. Brouwer, R. Roberts, T. Junker, H. Ghezel-Ayagh, J. Fuel Cell Sci. Technol. 4 (3) (2007).
[15] R. Kandepu, L. Imsland, B.A. Foss, C. Stiller, B. Thorud, O. Bolland, Energy 32 (4) (2007) 406–417.
[16] R. Roberts, J. Brouwer, F. Jabbari, T. Junker, H. Ghezel-Ayagh, J. Power Sources 161 (1) (2006) 484–491.
[17] C. Stiller, B. Thorud, O. Bolland, R. Kandepu, L. Imsland, J. Power Sources 158 (1) (2006) 303–315.
[18] J. Brouwer, F. Jabbari, E.M. Leal, T. Orr, J. Power Sources 158 (1) (2006) 213–224.
[19] F. Mueller, J. Brouwer, F. Jabbari, S. Samuelsen, J. Fuel Cell Sci. Technol. 3 (2) (2006) 144–155.
[20] R. Roberts, J. Brouwer, J. Fuel Cell Sci. Technol. 3 (18) (2006) 18–25.
[21] K. Min, J. Brouwer, J. Auckland, F. Mueller, S. Samuelsen, Dynamic Simulation of a Stationary PEM Fuel Cell System, ASME, Irvine, CA, 2006.
[22] F. Mueller, Design and Simulation of a Tubular Solid Oxide Fuel Cell System Control Strategy [Masters], University of California, Irvine, Irvine, 2005, p. 141.
[23] T. Kaneko, J. Brouwer, G.S. Samuelsen, J. Power Sources 160 (1) (2006) 316–325.
[24] F. Mueller, F. Jabbari, R. Gaynor, J. Brouwer, J. Power Sources 172 (1) (2007) 308–323.
[25] F. Mueller, F. Jabbari, J. Brouwer, T. Junker, H. Ghezel-Ayagh, Linear Quadratic Regulator for a Bottoming Solid Oxide Fuel Cell Gas Turbine Hybrid System, ASME, Newport Beach, CA, 2006.
[26] R. Roberts, A Dynamic Fuel Cell-Gas Turbine Hybrid Simulation Methodolgy to Establish Control Strategies and an Improved Ballance of Plant [Dissertation], University of California, Irvine, Irvine, 2005, p. 338.
[27] R.A. Roberts, B. Jack, E. Liese, R.S. Gemmen, J. Eng. Gas Turbines Power 128 (2006) 294–301.
[28] A.C. Burt, I.B. Celik, R.S. Gemmen, A.V. Smirnov, J. Power Sources 126 (1–2) (2004) 76–87.
[29] S. Campanari, P. Iora, J. Power Sources 132 (1–2) (2004) 113–126.
[30] M.R. Andrew, in: K.R. Williams (Ed.), An Introduction to Fuel Cells, Elsevier Publishing Company, New York, 1966.
[31] S. Srinivasan, O.A. Velev, A. Parthasarathy, D.J. Manko, A.J. Appleby, J. Power Sources 36 (3) (1991) 299–320.
[32] N.F. Bessette, Modeling and Simulation for Solid Oxide Fuel Cell Power Systems, Georgia Institute of Technology, Atlanta, 1994.
[33] J. Xu, G.F. Froment, AIChE J. 35 (1) (1989) 97–103.
[34] J. Xu, G.F. Froment, AIChE J. 35 (1) (1989) 88–96.
[35] P. Beckhaus, A. Heinzel, J. Mathiak, J. Roes, J. Power Sources 127 (1–2) (2004) 294–299.
[36] T.J. Pukrushpan, G.A. Stefanopoulou, P. Huei, in: J.M. Grimble, A.M. Johnson (Eds.), Modeling, Analysis, and Feedback Design, Springer, London, 2005.
[37] J.-W. Kim, A. Virkar, K.-Z. Fung, M. Karum, S. Singhal, J. Electrochem. Soc. 146 (1) (1999) 69–78.
[38] D. Brewer, Mater. Sci. Eng. A 261 (1–2) (1999) 284–291.
[39] D. Aquaro, M. Pieve, Appl. Therm. Eng. 27 (2–3) (2007) 389–400.
[40] M.L. Ferrari, L. Magistri, A. Traverso, A.F. Massardo, Control System for Solid Oxide Fuel Cell Hybrid Systems, 2005 June 6–9, 2005, ASME, Reno-Tahoe, Nevada, USA, pp. 1–9.
[41] F. Mueller, F. Jabbari, J. Brouwer, R. Roberts, T. Junker, H. Ghezel-Ayagh, Control Design for a Bottoming Solid Oxide Fuel Cell Gas Turbine Hybrid System, ASME, Irvine, CA, 2006.
[42] M.L. Ferrari, A. Traverso, L. Magistri, A.F. Massardo, J. Power Sources 149 (2005) 22–32.
[43] Y. Inui, N. Ito, T. Nakajima, A. Urata, Energy Convers. Manage. 47 (15–16) (2006) 2319–2328.
[44] R. Roberts, J. Brouwer, F. Jabbari, T. Junker, H. Ghezel-Ayagh, J. Power Sources 161 (2006) 484–491.
[45] A. Nakajo, C. Stiller, G. Harkegard, O. Bolland, J. Power Sources 158 (1) (2006) 287–294.
[46] R. Kandepu, L. Imsland, B.A. Foss, C. Stiller, B. Thorud, O. Bolland, Energy 32 (2007) 406–417.
[47] A. Selimovic, M. Kemm, T. Torisson, M. Assadi, J. Power Sources 145 (2) (2005) 463–469.